

# Two-Layer Thin Plate Temperature Control

Bilal A. Jarrah<sup>1</sup>, Dan Neculescu<sup>2</sup>, Malek Ali<sup>1</sup>, Anwar H. Al Assaf<sup>1</sup>

<sup>1</sup>Aircraft Maintenance Department, Faculty of Aviation Sciences, Amman Arab University, Amman, Jordan

<sup>2</sup>University of Ottawa/Department of Mechanical Engineering 770 King Edward Ave., Ottawa, ON, Canada

Received 3 Feb 2024

Accepted 27 Jun 2024

## Abstract

Utilizing the Laplace transform to derive the quadrupole model for both the direct and inverse problems, the temperature regulation of thin plate sides was examined. The polynomial expansions about poles and zeros are used to approximate the resultant hyperbolic functions. For multilayer plates, the open-loop and closed-loop control techniques were developed. The benefits and drawbacks of this method are demonstrated by simulation results for a two-layer plate. With this method, one may use the opposite side's temperature to regulate the temperature of one side of the plate in real time.

© 2024 Jordan Journal of Mechanical and Industrial Engineering. All rights reserved

**Keywords:** Inverse problem, Laplace transform, Thermal quadrupole, Polynomial expansion.

## Nomenclature

- L: Plate thickness[m].  
 $G_1$ : Direct problem transfer function.  
 $G_2$ : Inverse problem transfer function.  
 $\theta_1$ : The input temperature of the direct problem [ $^{\circ}\text{C}$ ].  
 $\theta_2$ : The output temperature of the direct problem [ $^{\circ}\text{C}$ ].  
 $\theta_{2d}$ : The desired temperature [ $^{\circ}\text{C}$ ].  
 $G_c$ : The Controller transfer function.  
 $k$ : The thermal conductivity [ $\frac{\text{m}^2}{\text{sec}}$ ].  
 $A$ : The amplitude of input temperature [ $^{\circ}\text{C}$ ].  
 $\Phi$ : The heat flux [ $\text{W}/\text{m}^2$ ].  
 $\alpha$ : The thermal diffusivity [ $\frac{\text{W}}{\text{m.K}}$ ].  
 $s$ : The complex variable.  
 $A_s$ : The area of the plane isothermal that is considered for the x-transfer [ $\text{m}^2$ ].  
 $\omega$ : The frequency [rad/sec].  
 IHCP: Inverse Heat conduction problem.  
 N: Number of terms for the direct problem.  
 M: Number of terms for the inverse problem.  
 PC: Personal computer.  
 $G_{dir} = G_1$ : Direct problem transfer function.  
 $G_{inv} = G_2$ : Inverse problem transfer function.

## 1. Introduction

Metal plate temperature regulation is necessary for a wide range of heat transfer applications. Applications include chemical reactors, heat exchangers, distillation

columns, heating plates, and furnaces for heating metal slabs. This calls for heating one surface to the appropriate temperature while maintaining the same temperature on the other. In the past, the problem could only be limited to measuring one side of the metal plate and calculating the temperature on the other. As a result, the entire temperature distribution over the thickness of the plate might be obtained by solving an inverse problem. This study looks at the more difficult problem of controlling plate temperature. According to Stolz [1], one of the earliest methods for solving inverse heat was this. In terms of the related direct problem's numerical inversion. He constructed the inverse problem. For tiny time increments, the Stolz solution seemed unstable nonetheless. While Miller et al. [2] and Murio initially provided regularized approaches [3] created a method called mollification that smooths the estimation of the surface temperature. With his method, the inverse problem is stabilized, and tiny time increments are permitted [4, 5]. Some studies computed the heat flow at one of the outer boundaries of the one-dimensional system using the Kalman smoothing approach [6, 7]. Bofeng Bai et al [8] created a simple method to estimate the two-dimensional heat conduction. A semi-finite body's temperature at one site, or a finite body's temperature at two locations, may be exploited by M. Monde to offer an analytical solution to the inverse heat by Laplace transform [9]. R. Pourgholi et al. [10] addressed the linear Inverse Heat Conduction Problem (IHCP) by Duhamel's principle to the matrix and using singular value decomposition. Numerous approaches to solving IHCP with various types of boundary conditions were presented by Cheng-Yu Ku, Edyta Hetmaniok et al., and Andrzej et al. [11, 12, and 13]. A book by Denis et al. describes how to solve the heat equation using integral transforms by using the thermal quadrupoles approach [14, 15]. For reconstructing the unknown heat

\* Corresponding author e-mail: b.jarrah@aau.edu.jo.

flow on the boundary in 2D and 3D scenarios, Adel Mhamdi and colleagues used a technique predicated on the interpretation of the frequency domain inverse heat control problem to solve the linear inverse heat conduction problem [16]. Xiaoshu and colleagues [17] presented an analytical method to study the transmission of heat in a composite slab subjected to cyclical temperature changes. Using the Laplace transform, Mitsutake et al. were able to analytically solve I H CPcases where there were far-field boundary conditions [18, 19].The 1D I H CPwere numerically solved by Mohammad et al. via the Tikhonov regularization approach. [20]. In order to solve a nonlinear heat conduction issue with temperature-dependent thermophysical properties, Guangjun Wang et al. employed the conjugate gradient technique and integrated heat flow measurement in the objective function [21, 22]. In order to translate the heat flow and temper on the front surface into those on the back surface, they first employed the Laplace transform to simplify the eq.by 3D to 1D via modal expansion [23]. A new closed-loop method for managing plate temperature using the inverse problem is presented by Necsulescu et al. [24-31].This work's main goal is to regulate a finite thin plate's surface temperature while heat from the opposite direction heats it up repeatedly. This is accomplished by solving the problem using the Laplace transform to create the quadrupole model equations and by utilizing an inverse problem formulation to create a temperature control loop.

**2. Formulating Problems**

With perfect interlayer contact, the temper Transm, through a wall of multi materials may be calculated for each layer using the thermal quadrupoles technique. The 1D heat conduction formula for the n-layer situation with perfect contact is as follows:

$$\frac{\partial^2 T}{\partial x^2} = \frac{1}{\alpha} \frac{\partial T}{\partial t} \tag{1}$$

Where is the H.F.

$$\phi = -k \frac{\partial T}{\partial x} \tag{2}$$

For the case of applying sinusoidal temperature variation  $\theta_1(0, t)$  on one side  $x=0$  and searching for the temperature of the other side  $\theta_2(L, t)$   $x=L$  as the boundary conditions are

$$\theta_1(0, t) = A \sin \omega t \theta_2(L, t) = free \tag{3}$$

$$\phi_1(0, t) = free \phi_2(L, t) = 0 \tag{4}$$

In the complex domain:

$$\frac{\partial^2 \theta}{\partial z^2} = \frac{s}{\alpha} \theta(z, s) \tag{5}$$

For n-layer plate using Quadrupole approach, the model is

$$(\theta_1 \phi_1) = M_1 M_2 \dots M_n (\theta_n \phi_n) \tag{6}$$

Where

$$\begin{aligned} M_1 &= [A_1 B_1 C_1 D_1] \\ M_2 &= [A_2 B_2 C_2 D_2] \\ M_n &= [A_n B_n C_n D_n] \end{aligned} \tag{6-1}$$

Where:

$$\begin{aligned} A_1 &= D_1 = \cosh \cosh(K_1 L_1) \\ B_1 &= \frac{1}{k_1 * K_1 * A_s} \sinh \sinh(K_1 L_1) C_1 \\ &= (K_1 * k_1 * A_s) \sinh(K_1 L_1) \end{aligned}$$

$$K_1 = \sqrt{\frac{s}{\alpha_1}}$$

For  $A_s$  is the plate surface area.

and:

$$\begin{aligned} A_2 &= D_2 = \cosh \cosh(K_2 L_2) \\ B_2 &= \frac{1}{k_2 * K_2 * A_s} \sinh \sinh(K_2 L_2) \\ C_2 &= (K_2 * k_2 * A_s) \sinh(K_2 L_2) \\ K_2 &= \sqrt{\frac{s}{\alpha_2}} \\ A_n &= D_n = \cosh \cosh(K_n L_n) \\ B_n &= \frac{1}{k_n * K_n * A_s} \sinh \sinh(n L_n) \\ C_n &= (K_n * k_n * A_s) \sinh(K_n L_n) \\ K_n &= \sqrt{\frac{s}{\alpha_n}} \end{aligned}$$

$L_1, L_2$  and  $L_n$  are the thicknesses of each layer and have it is specified diffusivity ( $\alpha_1, \alpha_2$  and  $\alpha_n$ ) for each layer.

Further results will be presented for a two-layer  $n=2$  case for simplifying the mathematical presentation.

**3. Simulation Model for a Two-layer Plate**

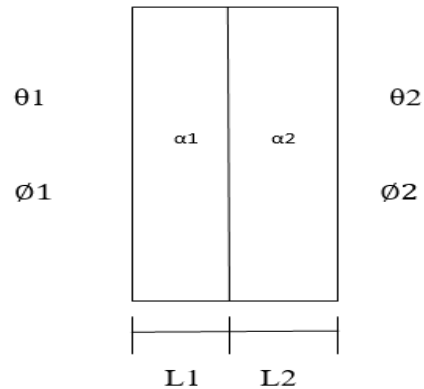


**Figure 1.** Material description in two layers.

The matrix for  $n=2$  layers is given by

$$M_1 * M_2 = [ABCD] \tag{7}$$

Where

$$A = A_1 * A_2 + B_1 * C_2$$

$$B = A_1 * B_2 + B_1 * D_2$$

$$C = C_1 * A_2 + D_1 * C_2$$

$$D = C_1 * B_2 + D_1 * D_2$$

This product will give

$$A = \cosh \cosh(K_1 L_1) \cosh \cosh(K_2 L_2) + \frac{K_2 k_2}{K_1 k_1} \sinh \sinh(K_1 L_1) \sinh(K_2 L_2)$$

$$B = \frac{1}{K_2 k_2 A_s} \cosh \cosh(K_1 L_1) \sinh \sinh(K_2 L_2) \frac{1}{K_1 k_1 A_s} \sinh \sinh(K_1 L_1) \cosh(K_2 L_2)$$

$$C = K_1 k_1 A_s \cosh(K_2 L_2) \sinh \sinh K_1 L_1 + K_2 k_2 A_s \cosh(K_1 L_1) \sinh \sinh(K_2 L_2)$$

$$D = \frac{K_1 k_1}{K_2 k_2} \sinh \sinh(K_1 L_1) \sinh \sinh(K_2 L_2) + \cosh \cosh(K_1 L_1) \cosh \cosh(K_2 L_2)$$

Such that

$$\theta_1 = A * \theta_2 + B * \phi_2 \tag{8}$$

$$\phi_1 = C * \theta_2 + D * \phi_2 \tag{9}$$

Solving these two equations gives  $G(s) = \frac{\theta_2}{\theta_1}$  as the temperature-dependent transfer function between the input and output temperatures.

For the boundary conditions (3) and (4), the results is

$$\frac{\theta_2}{\theta_1} = \frac{1}{A} \tag{10}$$

Where A is

$$A = \cosh \cosh(K_1 L_1) \cosh \cosh(K_2 L_2) + \frac{K_2 k_2}{K_1 k_1} \sinh \sinh(K_1 L_1) \sinh(K_2 L_2) \tag{11}$$

Given that

$$\begin{aligned} \cosh \cosh(x) \cosh \cosh(y) &= \frac{1}{2} [\cosh \cosh(x+y) + \cosh \cosh(x-y)] \\ \sinh(x) \sinh(y) &= \frac{1}{2} [\cosh \cosh(x+y) - \cosh \cosh(x-y)] \end{aligned}$$

Where

$$\begin{aligned} x &= K_1 L_1 \\ y &= K_2 L_2 \end{aligned}$$

A becomes

$$A = \frac{1}{2} [\cosh \cosh(x+y) + \cosh \cosh(x-y) + b \{ \cosh \cosh(x+y) - \cosh \cosh(x-y) \}] \tag{12}$$

where

$$b = \frac{K_2 k_2}{K_1 k_1}$$

**Case 1:** Same material and same thickness.

This will give

$$b = 1$$

Equation (10) becomes

$$A = \frac{1}{2} [\cosh \cosh(x+y) + \cosh \cosh(x-y)] \tag{13}$$

In case of the two layers' same thickness:

$$L_1 = L_2 = \frac{L}{2} \tag{14}$$

$$x = y = K \frac{L}{2} \tag{15}$$

Substitute for x and y in equation (11) gives

$$A = \frac{1}{2} \left[ \cosh \cosh \left( K \frac{L}{2} + K \frac{L}{2} \right) + \cosh \cosh \left( K \frac{L}{2} + K \frac{L}{2} \right) \right] \tag{16}$$

or

$$A = \cosh(KL) \tag{17}$$

**Case 2:** Different materials and same L of (L/2).

$$L_1 = L_2 = \frac{L}{2} \tag{18}$$

Such that for equation (13) and  $K_1 = \sqrt{\frac{s}{\alpha_1}}$  and  $K_2 = \sqrt{\frac{s}{\alpha_2}}$

$$x - y = \sqrt{s} \left[ \frac{L(\sqrt{\alpha_2} - \sqrt{\alpha_1})}{2\sqrt{\alpha_1 \alpha_2}} \right] = \sqrt{s} * AA \tag{19}$$

Where

$$AA = \left[ \frac{L(\sqrt{\alpha_2} - \sqrt{\alpha_1})}{2\sqrt{\alpha_1 \alpha_2}} \right] \tag{20}$$

and

$$x + y = \sqrt{s} \left[ \frac{L(\sqrt{\alpha_2} + \sqrt{\alpha_1})}{2\sqrt{\alpha_1 \alpha_2}} \right] = \sqrt{s} * BB \tag{21}$$

Where

$$BB = \left[ \frac{L(\sqrt{\alpha_2} + \sqrt{\alpha_1})}{2\sqrt{\alpha_1 \alpha_2}} \right] \tag{22}$$

Equation (10) becomes

$$A = \left[ \frac{1}{2} + \frac{b}{2} \right] [\cosh \cosh(\sqrt{s} * BB)] + \left[ \frac{1}{2} - \frac{b}{2} \right] [\cosh \cosh(\sqrt{s} * AA)] \tag{23}$$

Where

AA and BB are constants, not functions of s and

$$b = \frac{\sqrt{\alpha_1} k_2}{\sqrt{\alpha_2} k_1} \tag{24}$$

Equation (10) gives the Direct problem transfer function

$$G_1 = \frac{1}{A} = 1 / \left\{ \left[ \frac{1}{2} + \frac{b}{2} \right] [\cosh \cosh(\sqrt{s} * BB)] + \left[ \frac{1}{2} - \frac{b}{2} \right] [\cosh \cosh(\sqrt{s} * AA)] \right\} \tag{25}$$

While the inverse problem transfer function is:

$$G_2 = \frac{1}{G_1} = A = \left[ \frac{1}{2} + \frac{b}{2} \right] [\cosh \cosh(\sqrt{s} * BB)] + \left[ \frac{1}{2} - \frac{b}{2} \right] [\cosh \cosh(\sqrt{s} * AA)] \tag{26}$$

For the simulations, the transfer functions with hyperbolic functions from equation (25) and (26) were approximated about these approximations the poles  $p_1 p_2 \dots$  of direct problem ( $G_1$ ) and the zeros  $z_1 z_2 \dots$  of inverse problem ( $G_2$ ) as follows

$$\begin{aligned} G_1(s) &\approx 1 \\ &+ \left[ \frac{1}{2} + \frac{b}{2} \right] \frac{(s - p_1)(s - p_2)(s - p_3)(s - p_4)(s - p_5)(s - p_6) \dots}{p_1 p_2 p_3 p_4 p_5 p_6 \dots} \\ &+ \left[ \frac{1}{2} - \frac{b}{2} \right] \frac{(s - f_1)(s - f_2)(s - f_3)(s - f_4)(s - f_5)(s - f_6) \dots}{f_1 f_2 f_3 f_4 f_5 f_6 \dots} \end{aligned}$$

Where

$$p_n = - \left[ \frac{(2k-1)\pi}{2} * \frac{1}{BB} \right]^2, \quad n = 1, 2, 3, \dots, p_n$$

$$f_n = - \left[ \frac{(2k-1)\pi}{2} * \frac{1}{AA} \right]^2, \quad n = 1, 2, 3, \dots, p_n$$

and

$$\begin{aligned} G_2(s) &\approx \left[ \frac{1}{2} + \frac{b}{2} \right] \frac{(s - z_1)(s - z_2)(s - z_3)(s - z_4) \dots}{z_1 z_2 z_3 z_4 \dots} \\ &+ \left[ \frac{1}{2} - \frac{b}{2} \right] \frac{(s - y_1)(s - y_2)(s - y_3)(s - y_4) \dots}{y_1 y_2 y_3 y_4 \dots} \end{aligned}$$

Where

$$z_n = - \left[ \frac{(2k-1)\pi}{2} * \frac{1}{BB} \right]^2, \quad n = 1, 2, 3, \dots, z_n$$

$$y_n = - \left[ \frac{(2k-1)\pi}{2} * \frac{1}{AA} \right]^2, \quad n = 1, 2, 3, \dots, z_n$$

For both closed-loop and open loop methods, simulations were run. The closed-loop control block schematic is displayed, in Fig. (3), whereas the diagram for open-loop control is shown in Fig. (2).

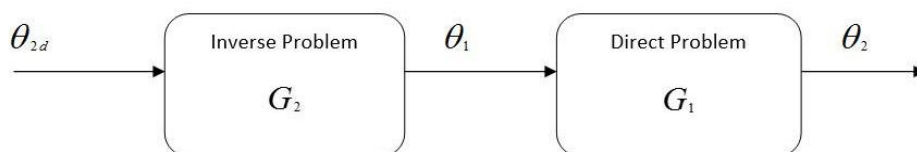


**Figure 2.** An open loop block schematic.

**4. Simulation Results**

Simulations were run using an aluminum (Al) alloy 2024 T6 with a thickness of  $L_2 = 0.015$  [m], and a thin Al plate with a  $L_1 = 0.015$  [m], thermal diffusivity  $\alpha_1 = 9.715e-5$

[m<sup>2</sup>/sec], and thermal conductivity  $k_1 = 237$  [w/m. K]. Thermal diffusivity  $\alpha_2 = 7.3e-5$  [m<sup>2</sup>/sec] and thermal conductivity  $k_2 = 177$  [w/m. K] for the second layer for two two-layer cases. Multiple values of the  $\omega$  sinusoidal input were tested, along with the truncated transfer functions and some sample values of  $M = 4$  zeros and  $N = 8$  poles.

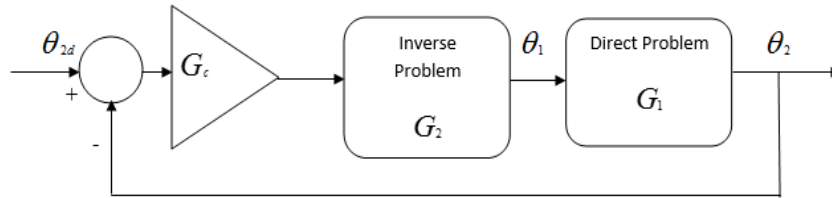
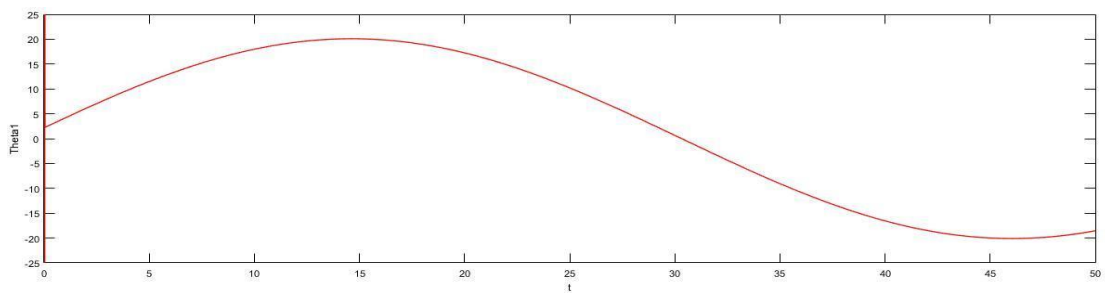
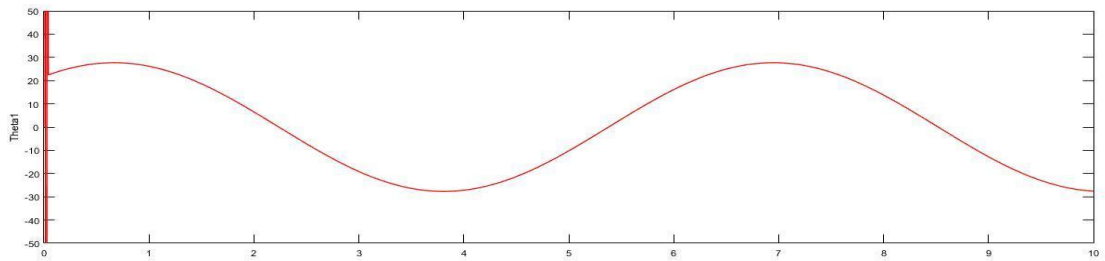


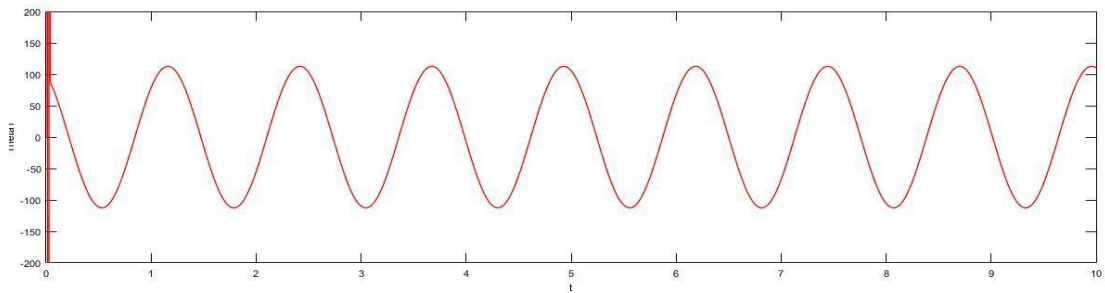
**Figure 3.** Block schematic of a closed loop.  $\theta_{2d}$  is the desired value of  $\theta_2$  and  $G_c$  is the closed-loop control law.



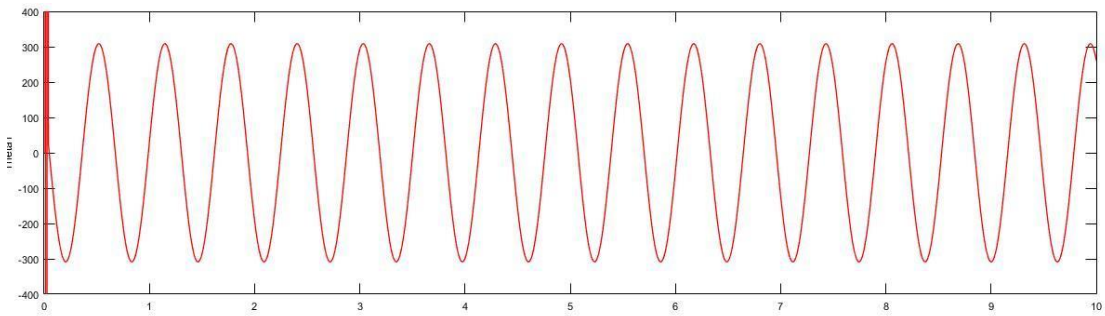
A



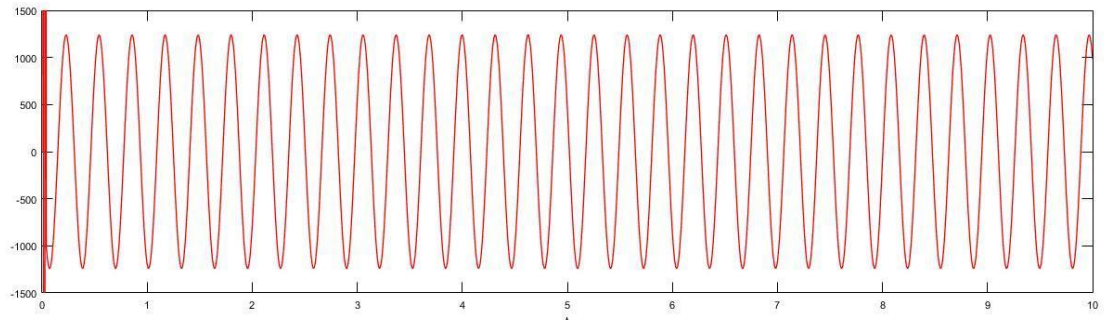
B



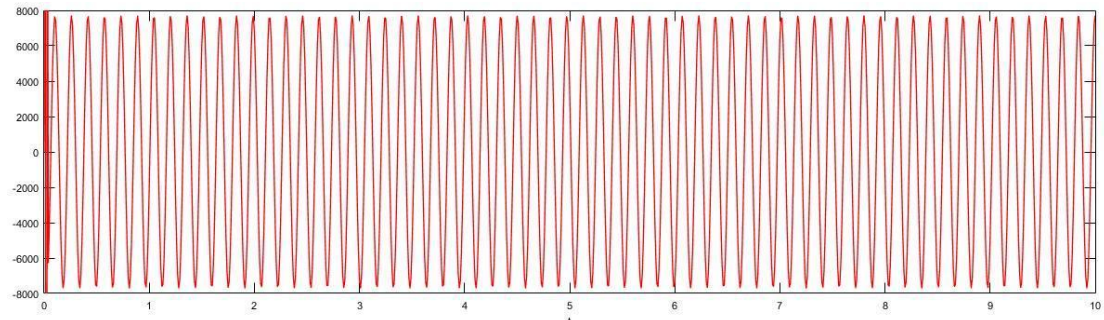
C



D

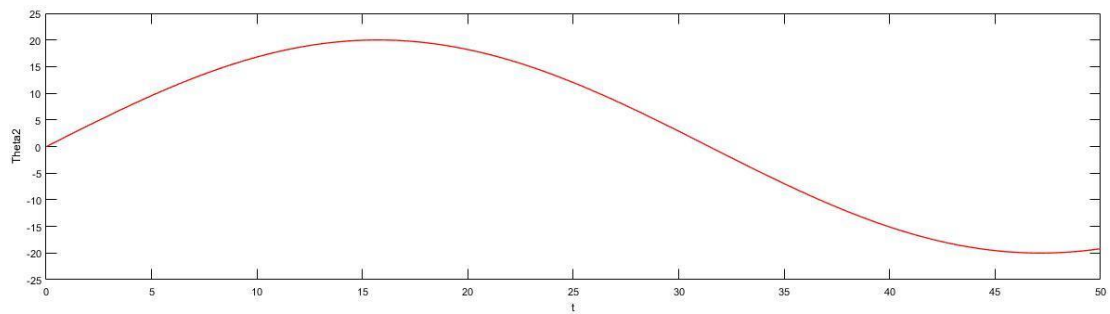


E

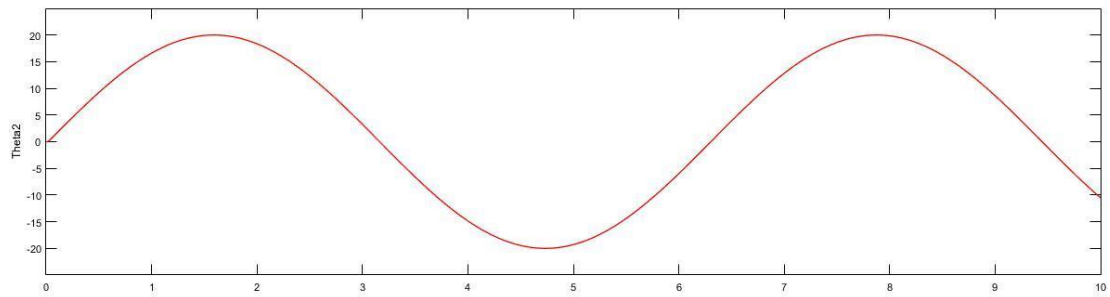


F

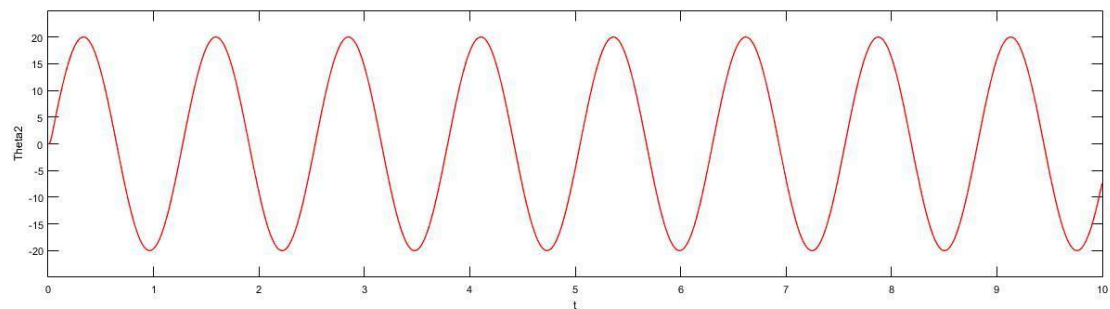
Figure 4. Open loop response  $\theta_1$  for the Inverse problem with  $N = 8$ ,  $M = 4$ , and  $\omega =$  (A) 0.1, (B) 1, (C) 5, (D) 10, (E) 20, and (F) 40 radian/second



A



B



C

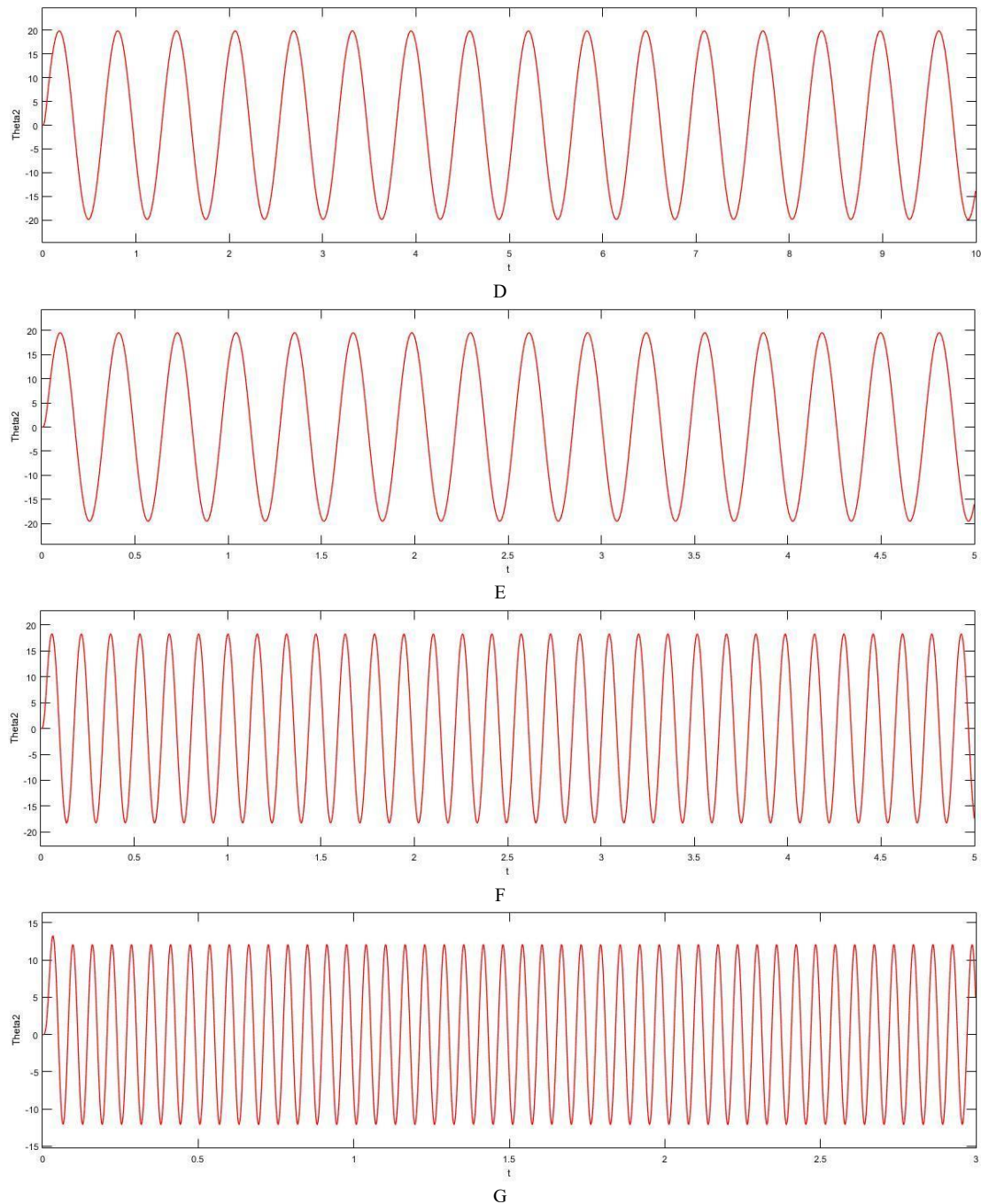
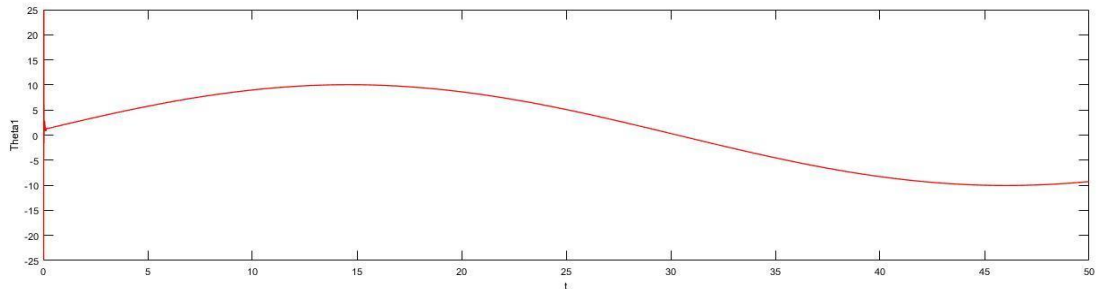


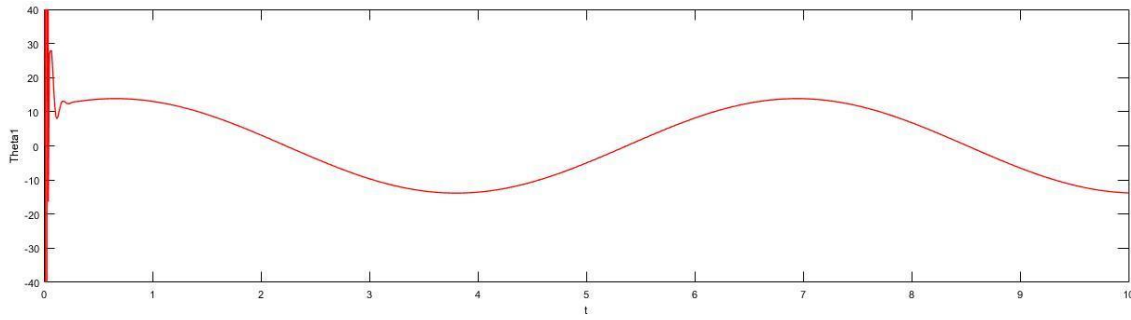
**Figure 5.**  $\theta_2$  response of an open loop control system with  $N = 8$ ,  $M = 4$ , and  $\omega =$ (A) 0.1, (B) 1, (C) 5, (D) 10, (E) 20, (F) 40, and (G) 100 radian/second.

From Figure 4 (A - F) we can see that the response to the inverse problem is increasing with frequency but at a slower speed than we see in the single-layer case due to different types of material for the second layer. Figures 5 (A–E) show

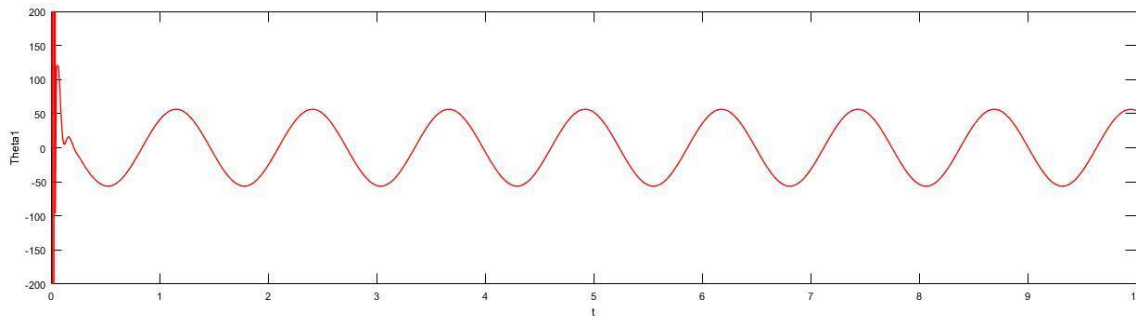
that the system response is nearly identical to the intended value, but Figures 5 (F&G) show that the response begins to fall with increasing frequency.



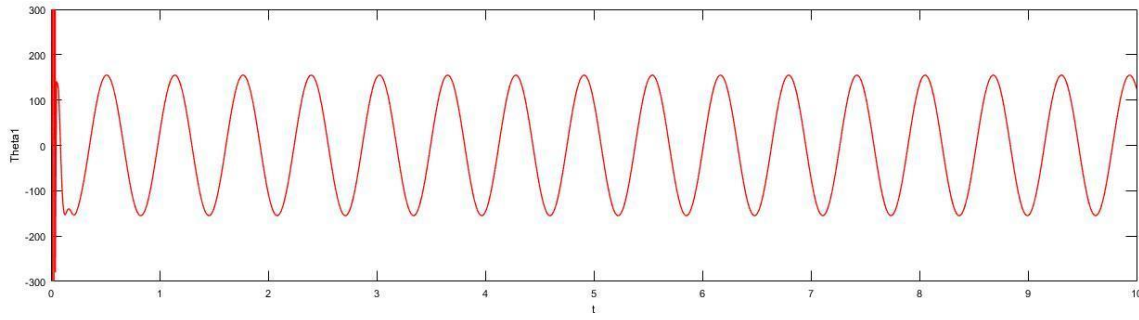
A



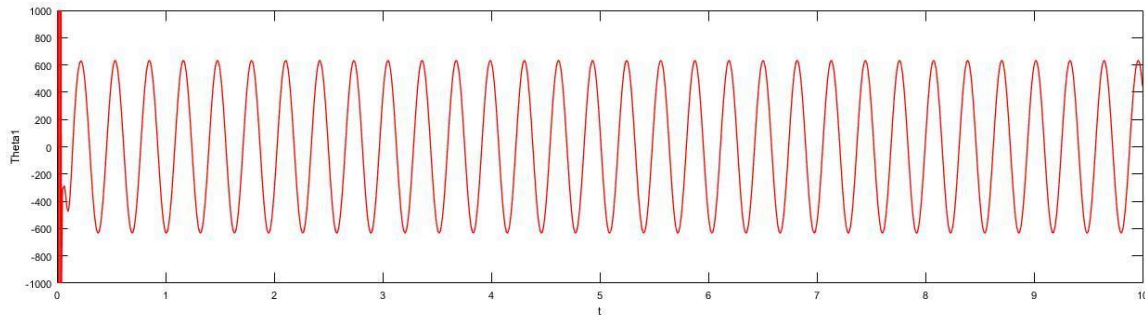
B



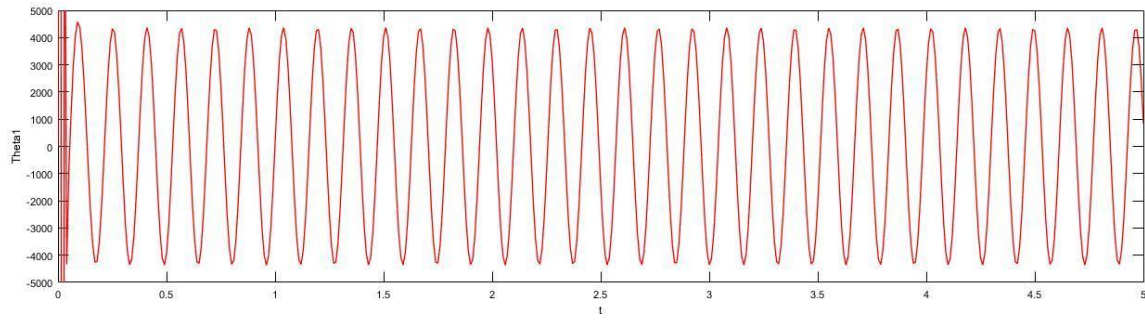
C



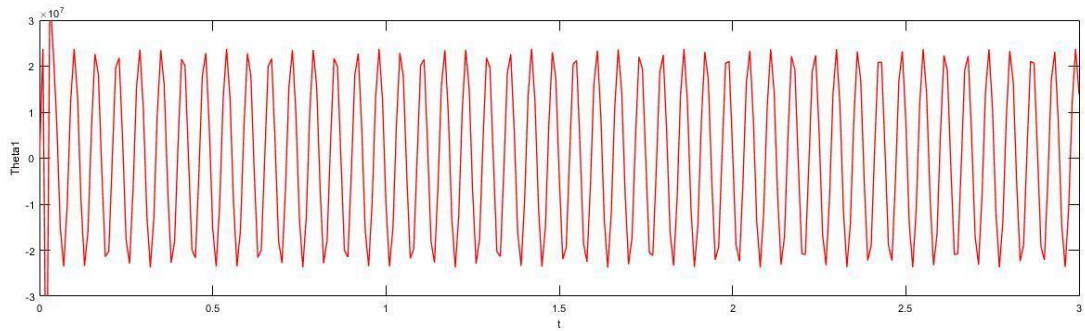
D



E

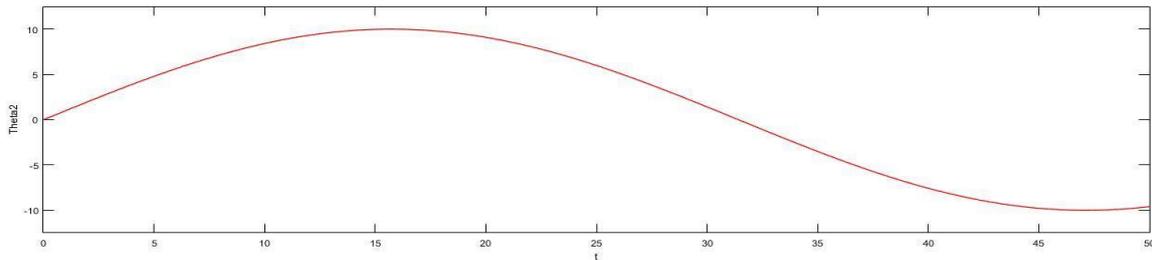


F

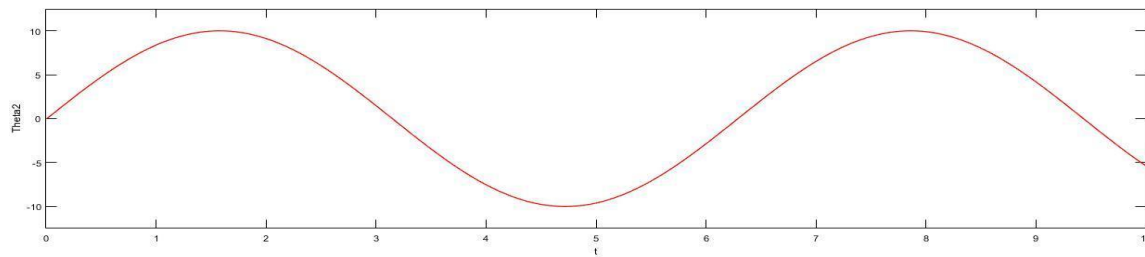


G

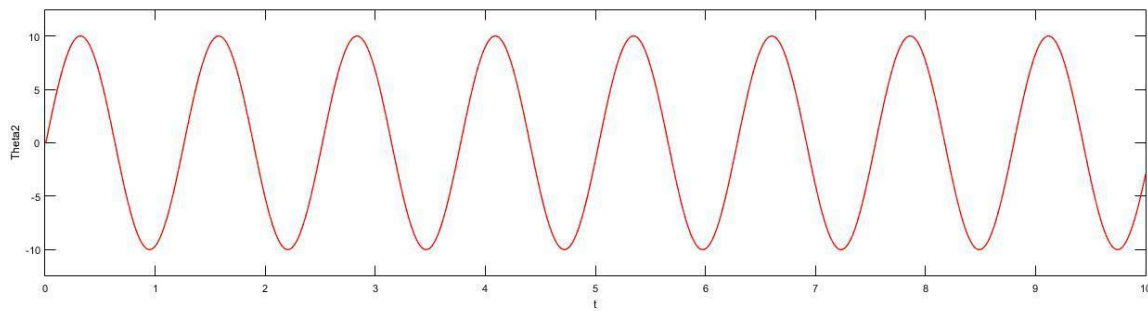
**Figure 6.** Closed loop response  $\theta_1$  for the inverse problem with  $N=6$ ,  $\alpha=1$ ,  $M=4$ , and  $\omega =$  (A) 0.1, (B) 1, (C) 5, (D) 10, (E) 20, (F) 40, and (G) 100 radian/second.



A



B



C

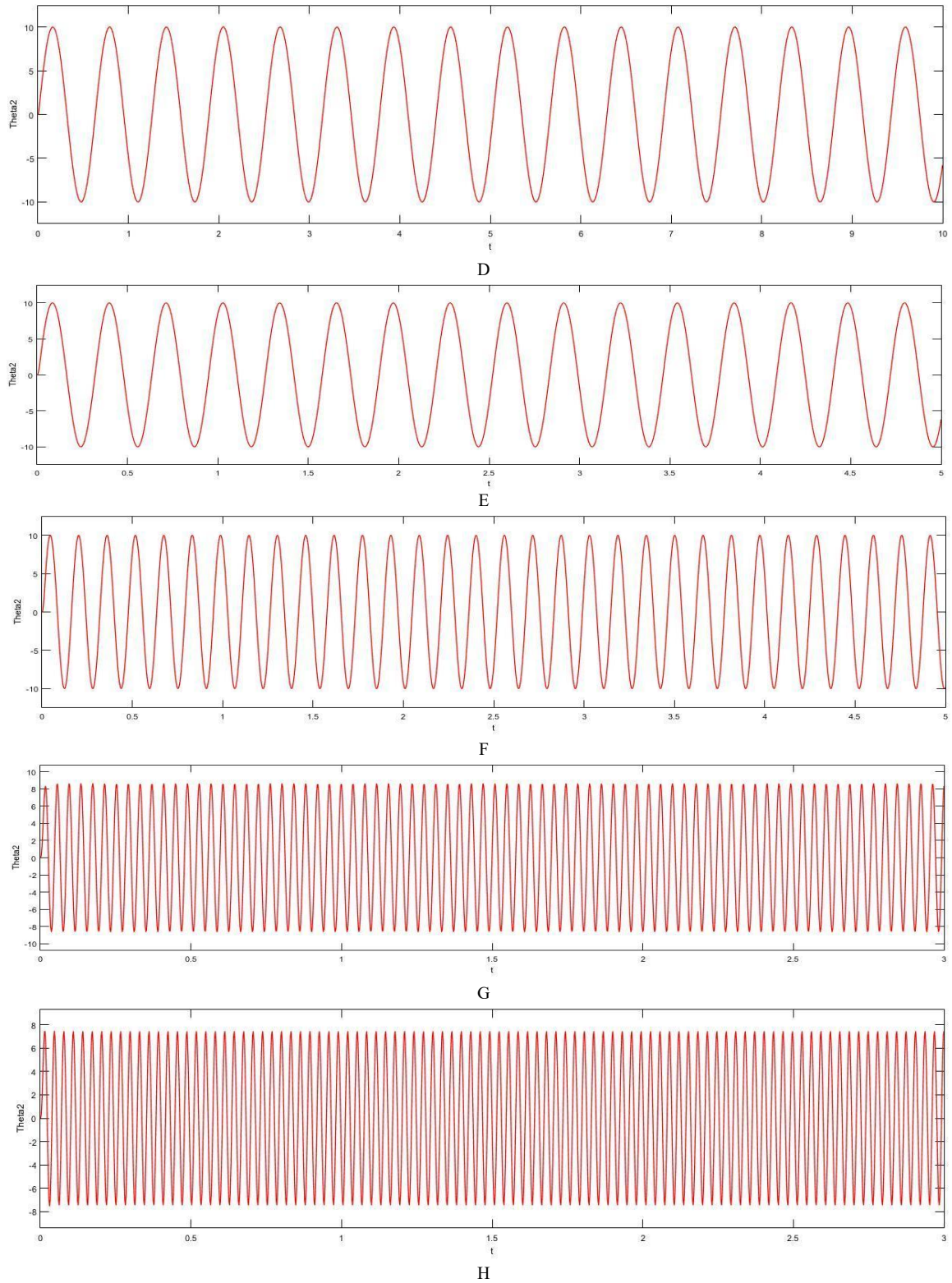
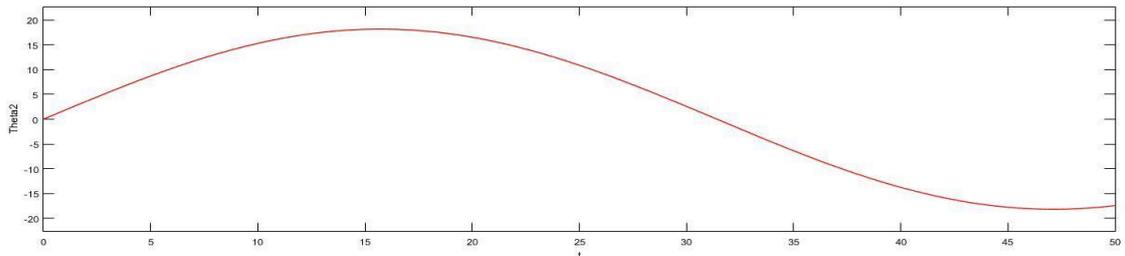
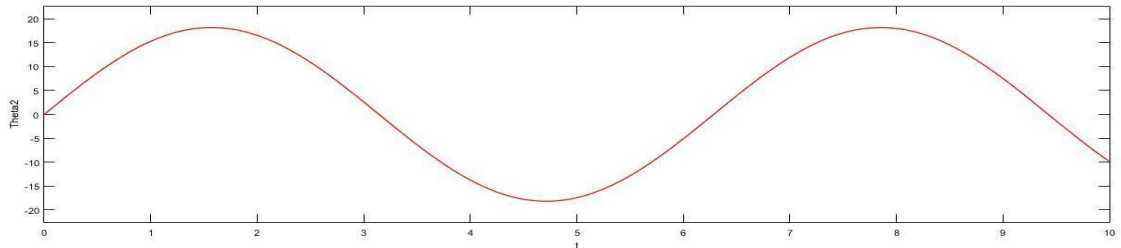


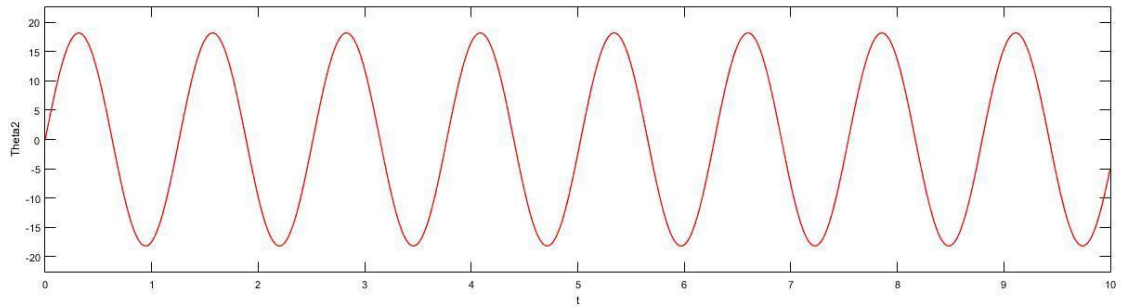
**Figure 7.** Shows the  $\theta_2$  response of the closed loop control for  $N = 6$ ,  $M = 4$ , and  $\omega =$  (A) 0.1, (B) 1, (C) 5, (D) 10, (E) 20, (F) 40, (G) 160, and (H) 200 radian/second.



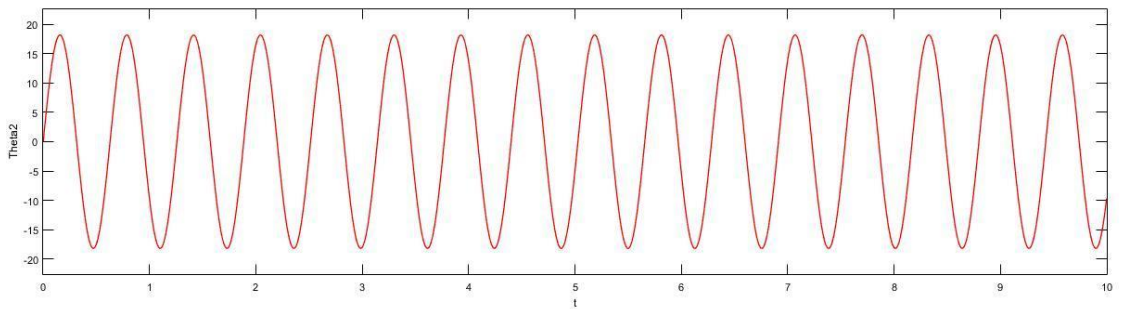
A



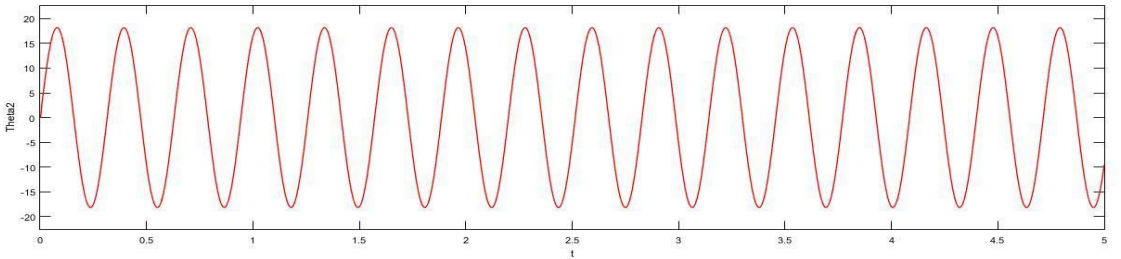
B



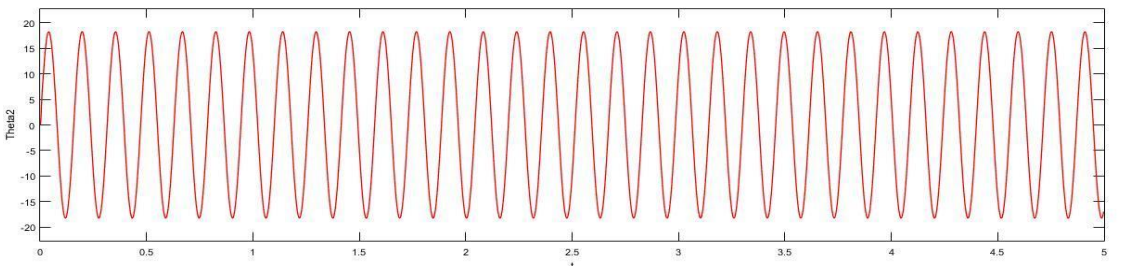
C



D



E



F

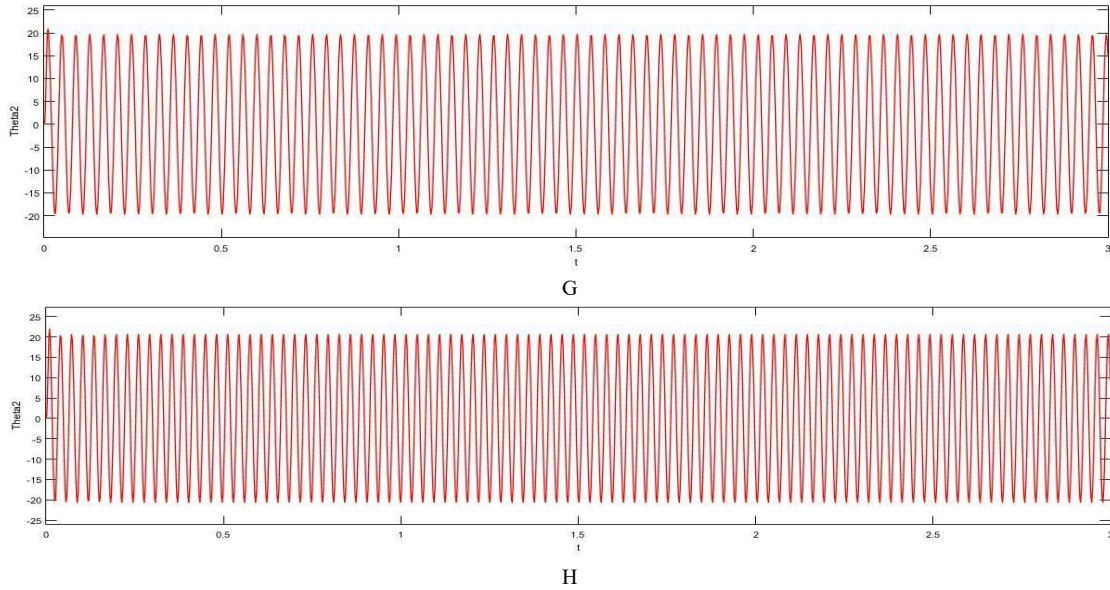


**Figure 8.** Closed-loop control response  $\theta_2$  for  $N = 6, = 10, M = 4, ,$  and for  $\omega =$  (A) 0.1, (B) 1, (C) 5, (D) 10, (E) 20, (F) 40, (G) 160, and (H) 200 radian/second. While the inverse response grows extremely quickly in the final figure (6-G), Figure 6(A-F) shows that the response to the inverse problem increases with the frequency increase. The system response is half of the intended value, as predicted, from Figure 7(A-F). This is because of the gain value of one. However, Figure 7(G-H) shows that the response value starts to drop with increasing frequency.

Figure 8 ( A - H) on the other hand shows how we can always bring the response value close to the desired value by using a gain value of (10) which is acceptable and keeps the system stable.

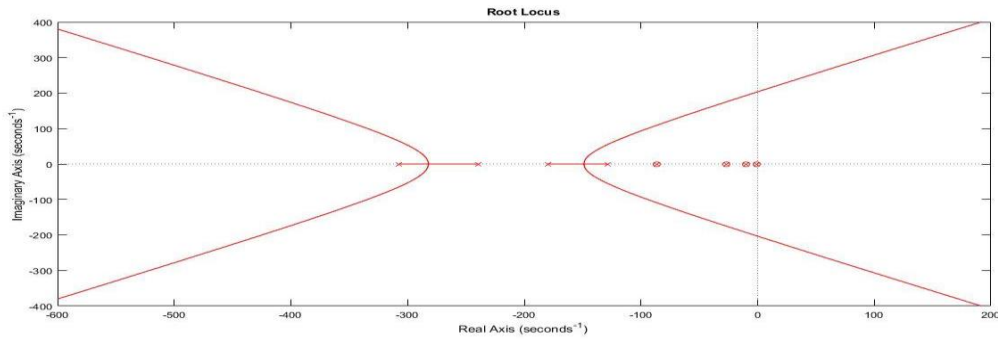


**Figure 9.** Plotting the root locus for  $N = 8,$  and  $M = 4.$

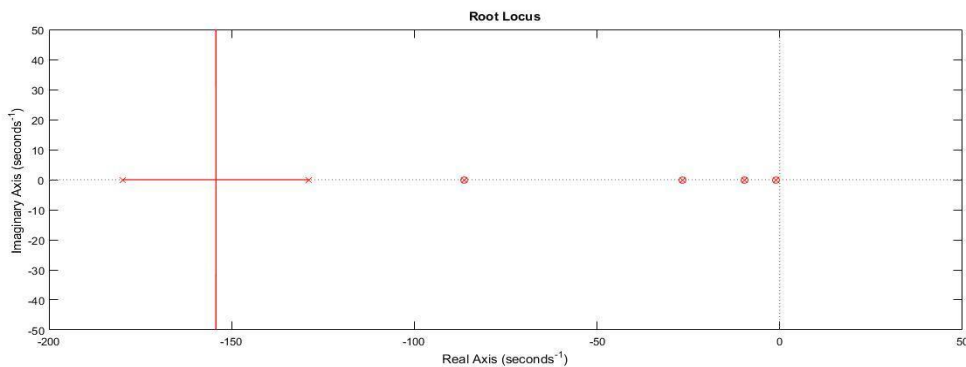


**Figure 10.** Plotting the root locus for  $N = 6,$  and  $M = 4.$

From Figures ( 9 & 10) we see that the number of terms is the major factor for the stability of the system, as we can see from Figure (9) the system is stable only for a gain value

up 4.43 where the curve intersects imaginary axis, while figure (10) shows that the system is always stable for any gain value.

## 5. Conclusion

The suggested method, which is based on the solution of an inverse problem, allows the temperature on one face of a plate to be regulated in real-time to the other face's desired value. The outcomes of the simulation show the benefits and drawbacks of this method. Polynomial expansions are used to approximate the resultant hyperbolic functions. The closed-loop strategy has a longer frequency bandwidth than the open-loop approach, according to the data. Because truncated polynomials are used, the suggested methodology differs from other regularization techniques for ill-posed problems and is especially well-suited for real-time temperature management. This approach must be further investigated for multilayer plates and verified through experiments.

## References

- [1] G. Stolz, "Numer. Solu. to an Inve. Problem of Heat Conduction for Simple Shapes." *J. Heat Transfer* Vol. 82, No. 1, 1960, 20-25.
- [2] K. Miller, "Stabilized quasi-reversibility and other nearly-best-possible methods for non-well posed problems". In *Symposium on Non-Well-Posed Problems and Logarithmic Convexity* Springer, 1973, 161-176.
- [3] D. A. Murio, "The Mollification Method". *Computers Math. Applic.* Vol. 17, No. 10, 1989, 1385-1396.
- [4] Moh'd et al, "Application of Neural Net Modeling and Inverse Control to the Desulphurization of Hot Metal Process". *Jordan Journal of Mechanical and Industrial Engineering*, Vol. 1, No. 2, 1989, 79-84.
- [5] Wen-Guang LI, "Inverse Design of Impeller Blade of Centrifugal Pump with a Singularity Method". *Jordan Journal of Mechanical and Industrial Engineering*, Vol. 5, No. 2, 2011, 119-128.
- [6] Nejla Gaaloul, Naouel Daouas, "An extended approach of a Kalman smoothing technique". *Inter.J. of Ther. Scie.*, Vol. 134, 2018.
- [7] S. Shawish et al, "CFD Simulation of Energy Transfer within a Membrane Heat Exchanger under Turbulent Flow". *Jordan Journal of Mechanical and Industrial Engineering*, Vol. 17, No. 2, 2023, 139-154.
- [8] Bofeng Bai et al, "A Solution to the Two-Dimensional Inverse Heat Conduction Problem". *Heat Transfer—Asian Research*, Vol. 29, No. 2, 2000, 113-119.
- [9] Masanori Monde et al, "Analytical Approach with Laplace Transformation to the Inverse Problem of One Dimensional Heat Conduction". *Heat Transfer-Asian Research*, Vol. 32, No. 1, 2003, 29-41.
- [10] R. Pourgholi et al, "A Duhamel Integral Based Approach to Identify an Unknown Radiation Term in a Heat Equation with Non-linear Boundary Condition". *Appl. Appl. Math.* Vol. 7, No. 1, 2012, 52-70.
- [11] Cheng-Yu Ku et al, "On Solving Two-Dimensional Inverse Heat Conduction Problems". *Appl. Sci.*, Vol. 9, 2019, 1-21.
- [12] Edyta Hetmaniok et al, "Solution of the inverse heat conduction problem with Neumann boundary condition by using the Hom.Pertur. method". *Thermal Scie.* Vol. 17, No. 3, 2013, 643-650.
- [13] Andrzej et al, "Iterative algorithm for solving the inverse heat conduction problems with the unknown source function". *Inve. Prob. in Scie. & Eng.*, Vol. 23, No. 6, 2015, 1056-1071.
- [14] Denis et al, "Thermal Quadrupoles: Solving the Heat Equation through Integral Transforms". John Wiley, 2000.
- [15] Fadi A. Ghaith et al, "Dynamic Modeling and Control of Elastic Beam Fixed on A Moving Cart and Carrying Lumped Tip". *Jordan Journal of Mechanical and Industrial Engineering*, Vol. 5, No. 1, 2011, 61-70.
- [16] Adel Mhamdi et al, "Formulation, and Solution of Multidimensional Inverse Heat Conduction problems". *Numer. Heat transfer*, Vol. 47, No. 6, 2005, 111 - 133.
- [17] Xiaoshu Lü et al, "Transient heat conduction in the composite slab-Analytical method". *J. of Phys. A*, vol. 38, 2005, 81 - 96.
- [18] Mitsutake et al, "Improved analytical solution for inverse heat conduction problems". *Inter. J. of Heat & Mass Tran.*, Vol. 49, 2006, 2864 - 2876.
- [19] Bahaa et al, "A Neural Network Based Real Time Controller for Turning Process". *Jordan Journal of Mechanical and Industrial Engineering*, Vol. 1, No. 1, 2007, 43-55.
- [20] Mohammad et al, "Solving inverse heat conduction problems by using Tikhonov regularization in combination with the genetic algorithm". *amcejournal*, Vol. 3, 2021, ISSN: 2766-9823.
- [21] Guangjun Wang et al, "A multiple model adaptive inverse method for nonlinear heat transfer system with temperature-dependent thermophysical properties". *Int. J. Heat Mass Transf.* Vol. 118, 2018, 847-856.
- [22] Rashid Ali et al, "Numerical Study of Fluid Dynamics and Heat Transfer Characteristics for the Flow Past a Heated Square Cylinder". *Jordan Journal of Mechanical and Industrial Engineering*, Vol. 15, No. 4, 2021, 357-376.
- [23] Zaichun et al, "Estim. of front surface temp. and heat flux of a locally heated plate". *Inter.J. of Heat and Mass Transfer*, Vol. 54, 2011, 3431 - 3439.
- [24] Neculescu et al, Closed - loop control of plate temperature using inverse problem, 13th Inter. Conf. on Infor.in Control, Automation and Robotics, 421-425, 2016, Lisbon, Portugal.
- [25] M. Ababneh et al, "Variable Structure Controller Schemes Based on Work and Energy Principle for SIMO Systems". *Journal of Mechanical and Industrial Engineering*, Vol. 5, 2011, 407-417.
- [26] Kalaivani et al, "Hybrid DEBBO Algorithm for Tuning the Parameters of PID Controller Applied to Vehicle Active Suspension System". *Jordan Journal of Mechanical and Industrial Engineering*, Vol. 9, No. 2, 2015, 85-102.
- [27] Abdesselem Chikhi, "Direct Torque Control of Induction Motor". *Journal of Mechanical and Industrial Engineering*, Vol. 8, 2014, 169-176.
- [28] Mayouf Messaoud et al, "Sensorless Control System Design of a Small Size Vertical Axis Wind Turbine". *Jordan Journal of Mechanical and Industrial Engineering*, Vol. 12, No. 2, 2018, 93-98.
- [29] J. Al-Nabulsi et al, "Automatic Control of Electrodes in Lithotripsy Machine". *Jordan Journal of Mechanical and Industrial Engineering*, Vol. 3, No. 3, 2009, 93-98.
- [30] Anwar Hamdan Al-Assaf et al, "PID Power Controller to a Setpoint of Fluid Level Height in a Reservoir for Unattended Human Monitoring". *Int. J. Electr. Electron. Eng. Stud.*, Vol. 8, No. 3, 2021, 1-13.
- [31] Odi Fawwaz Aalrebei et al, "Lightweight Methane-Air Gas Turbine Controller and Simulator". *Energy Conversion and Management*, Vol. 15, 2022, 100242.